Analysis of Spin-1/2 Particle Scattering in a Spinning Cosmic String Spacetime with Torsion, Curvature, and a Coulomb Potential

Abdelmalek Boumali*

Laboratory of theoretical and applied Physics

Echahid Cheikh Larbi Tebessi University, Algeria

(Dated: November 24, 2025)

This paper investigates the scattering states of spin-(1/2) particles in the spacetime of a spinning cosmic string with spacelike disclination and dislocation, with and without a Coulomb interaction. Working within the tetrad formalism, we solve the Dirac equation for several configurations of angular momentum density J_t and the torsion parameter J_z that are relevant from a physical perspective. These configurations include balanced torsion ($J_t = J_z$), pure spinning strings ($J_z = 0$), pure screw dislocations ($J_t = 0$) and the general case. In all cases, the geometry modifies an effective azimuthal quantum number, and for strong rotation it introduces a geometric radial cutoff ρ_c that acts as a hard wall. These factors lead to closed-form expressions for the radial wave functions, phase shifts and differential cross sections, which are expressed in terms of confluent hypergeometric and Bessel functions. We demonstrate that conical curvature, rotation and torsion generate Aharonov–Bohm–like contributions, as well as energy- and momentum-dependent asymmetries in Dirac–Coulomb scattering. This results in topology-renormalised Mott/Rutherford patterns. In the Coulomb-free limit, scattering becomes purely geometric yet still exhibits characteristic forward enhancement, which is governed by defect parameters and the cutoff. We briefly discuss possible realisations in Dirac materials, such as strained or defective graphene, where lattice disclinations and dislocations mimic the cosmic-string geometry.

PACS numbers: 04.62.+v; 04.40.−b; 04.20.Gz; 04.20.Jb; 04.20.−q; 03.65.Pm; 03.50.−z; 03.65.Ge; 03.65.−w; 05.70.Ce

Keywords: Spinning cosmic string, Spin-1/2 particles, Curvature (disclination),Torsion (dislocation), Quantum fields theory in curved spacetime

* boumali.abdelmalek@gmail.com

I. INTRODUCTION

Topological defects, such as cosmic strings, are hypothetical remnants of symmetry-breaking phase transitions in the early universe as predicted by grand unified theories. They induce conical curvature (disclination), which is characterised by an angular deficit α, and when they are endowed with intrinsic spin or lattice-like distortions, they may also carry torsion/dislocation, which is encoded by rotation and screw-dislocation parameters (J_t and J_z). In cylindrical coordinates, these geometric features enter Dirac theory via the tetrad and spin connection. In strongly rotating regimes, they can generate a geometry-induced lower radial bound ρ_c that excludes non-causal regions and acts as a hard-wall boundary. Consequently, the partial-wave indices, phase shifts and scattering observables for spin-$(1/2)$ particles are all modified by the underlying spacetime structure.

Most previous investigations of fermions in cosmic-string backgrounds have focused on bound states and spectral properties, demonstrating the effects of the angular deficit and torsion on Dirac energy levels, effective centrifugal barriers, and spin–orbit couplings. In contrast, scattering states which directly encode observable cross sections and potential signatures of strings in astrophysical or analogue condensed-matter settings have received considerably less attention, especially when combined with long-range Coulomb fields. However, in realistic scenarios, charged sources or electromagnetic fields are expected to coexist with string-like defects and their interaction with curvature, rotation and torsion can generate distinctive diffraction patterns and phase-shift structures that are not captured by bound-state analyses alone [1–14].

The main goal of this paper is to provide a unified, analytical description of Dirac scattering in a spinning cosmic-string spacetime with spacelike disclination and dislocation, with and without a static Coulomb potential. We demonstrate how the geometry reshapes scattering through two key factors [15–17]:

(i) an effective azimuthal quantum number $\kappa_{eff}(\alpha, J_t, J_z; E, k)$ that incorporates the conical angle, rotation, torsion and the energy–momentum of the particle; and

(ii) a geometric cutoff ρ_c, which is activated in strongly rotating regimes and introduces additional boundary-induced phases. Together, these quantities control the partial-wave phase shifts and thus the differential and total cross sections.

To clarify the function of each geometric parameter, we analyse several physically relevant configurations: the pure cosmic string ($J_t = J_z = 0$), the balanced torsion case ($J_t = J_z$), the pure spinning string ($J_z = 0$), the pure screw dislocation ($J_t = 0$), and the fully general case with both J_t and J_z non-zero. For each configuration, we derive the radial Dirac equations using the tetrad formalism and solve them in closed form: confluent hypergeometric functions describe the Coulomb problem, while Bessel functions describe purely geometric scattering. This enables us to derive explicit expressions for the phase shifts, scattering amplitudes and cross sections and to determine how conical curvature, rotation, torsion and the cutoff ρ_c generate Aharonov–Bohm–like contributions and energy- or momentum-dependent asymmetries. Additionally, we briefly discuss possible realisations in Dirac materials, such as strained or defective graphene and Dirac/Weyl semimetals, where lattice disclinations and dislocations can mimic the cosmic-string geometry and render the predicted scattering effects accessible to experimentation.

For clarity, the paper is organised as follows. Section II introduces the spinning cosmic-string metric with spacelike disclination and dislocation, reviews the tetrad formalism and derives the Dirac equation in cylindrical coordinates. This section highlights the emergence of κ_{eff} and the geometric cutoff ρ_c. Section III treats Dirac scattering in the presence of a Coulomb potential. It analyses the pure string, balanced torsion, pure spinning, screw-dislocation and general cases in detail, deriving the corresponding radial solutions and phase shifts. Section IV focuses on geometric scattering in the absence of the Coulomb interaction, emphasising the purely topological contributions to the scattering amplitude. Section V presents and compares the angular distributions and total cross sections for all configurations, illustrating how curvature, rotation, torsion and the cutoff modify the Mott/Rutherford patterns and the Coulomb-free diffraction structures. Section VI discusses potential experimental implementations in graphene and other Dirac materials, where analogue cosmic-string geometries may be engineered. Finally, Section VII summarises our main results and outlines possible extensions, including additional interactions and dynamical string backgrounds.

II. DIRAC EQUATION IN THE COSMIC STRING BACKGROUND

In this section, we address the solution of the Dirac oscillator in the presence of a cosmic string background characterized by the spacetime signature $(-+++)$. The geometry induced by the cosmic string is described using cylindrical coordinates (t, ρ, ϕ, z), and the corresponding line element for a straight, rotating cosmic string endowed with torsion is given by [15–17]:

$$ds^2 = -\left(dt + 4GJ^t d\varphi\right)^2 + d\rho^2 + \alpha^2\rho^2 d\varphi^2 + \left(dz + 4GJ^z d\varphi\right)^2, \tag{1}$$

where the parameter α, satisfying $0 < \alpha < 1$, represents the angular deficit associated with the conical geometry. The quantity J^t denotes the linear density of angular momentum, responsible for frame-dragging effects, while J^z characterizes the screw-dislocation parameter linked to torsion.

The coordinate ranges are defined as $-\infty < t, z < \infty$, $0 \leq \rho < \infty$, and $0 \leq \phi \leq 2\pi$. The deficit parameter α is associated with the conical structure of the spacetime and satisfies the relation $\alpha = 1 - 4\mu$, where μ is the linear mass density of the cosmic string expressed in natural units.

The metric tensor $g_{\mu\nu}$ in matrix form is:

$$g_{\mu\nu} = \begin{pmatrix} -1 & 0 & -4GJ^t & 0 \\ 0 & 1 & 0 & 0 \\ -4GJ^t & 0 & \alpha^2\rho^2 - 16G^2[(J^t)^2 - (J^z)^2] & 4GJ^z \\ 0 & 0 & 4GJ^z & 1 \end{pmatrix} \tag{2}$$

We note here that for the metric in Eq. (1), the azimuthal component is $g_{\phi\phi} = \alpha^2\rho^2 - 16G^2[(J_t)^2 - (J_z)^2]$. Physical admissibility requires $g_{\phi\phi} > 0$ to ensure a positive definite metric signature and avoid closed timelike curves or unphysical regions[18, 19]. Hence, when $(J_t)^2 > (J_z)^2$, we restrict the configuration space to

$$\rho > \rho_c = \frac{4G}{\alpha}\sqrt{(J_t)^2 - (J_z)^2}. \tag{3}$$

For $J_z = 0$, this reduces to $\rho > 4G|J_t|/\alpha$; for $J_t = 0$, the inequality is automatically satisfied for all $\rho > 0$.

This radial cutoff ρ_c has important implications for the quantum system. All normalization integrals for the wavefunctions are thus evaluated over $\rho \in (\rho_c, \infty)$ (or $(0, \infty)$ when $\rho_c = 0$), ensuring that the probability density is confined to the physically admissible region. Boundary conditions at $\rho = \rho_c$ are imposed such that the wavefunction vanishes or satisfies the conditions that prevent leakage into the forbidden zone, analogous to hard-wall potentials in defect spacetimes. This restriction modifies the effective centrifugal barrier in the radial equation, potentially shifting the energy levels and altering the density of states. In particular, for large torsion parameters, ρ_c introduces a minimal radius that lifts low-angular-momentum degeneracies and affects the ground-state energy, providing a geometric regularization akin to those in rotating frames [18, 19].

Now, the physical properties of this spacetime are determined by the value of $j^2 = (J^t)^2 - (J^z)^2$ [16]:

- Case (1): $j^2 = 0$ (i.e., $|J^z| = |J^t|$)

$$ds^2 = -\left(dt + 4GJ\, d\varphi\right)^2 + d\rho^2 + \alpha^2\rho^2 d\phi^2 + \left(dz + 4GJ\, d\varphi\right)^2 \tag{4}$$

  with

$$g_{\mu\nu} = \begin{pmatrix} -1 & 0 & -4GJ^t & 0 \\ 0 & 1 & 0 & 0 \\ -4GJ^t & 0 & \alpha^2\rho^2 & 4GJ^z \\ 0 & 0 & 4GJ^z & 1 \end{pmatrix} \tag{5}$$

  This describes a string interacting with a circularly polarized plane-fronted gravitational wave.

- Case (2): $|J^z| = 0$

$$ds^2 = -\left(dt + 4GJ^t d\varphi\right)^2 + d\rho^2 + \alpha^2\rho^2 d\varphi^2 + dz^2 \tag{6}$$

  with

$$g_{\mu\nu} = \begin{pmatrix} -1 & 0 & -4GJ^t & 0 \\ 0 & 1 & 0 & 0 \\ -4GJ^t & 0 & \alpha^2\rho^2 - 16G^2(J^t)^2 & 0 \\ 0 & 0 & 0 & 1 \end{pmatrix} \tag{7}$$

  This corresponds to a spinning cosmic string without any spatial dislocation.

- Case (3): $|J^t| = 0$

$$ds^2 = -dt^2 + dr^2 + \alpha^2\rho^2 d\varphi^2 + \left(dz + 4GJ^z d\varphi\right)^2 \tag{8}$$

with

$$g_{\mu\nu} = \begin{pmatrix} -1 & 0 & 0 & 0 \\ 0 & 1 & 0 & 0 \\ 0 & 0 & \alpha^2\rho^2 + 16G^2(J^z)^2 & 4GJ^z \\ 0 & 0 & 4GJ^z & 1 \end{pmatrix} \tag{9}$$

In this scenario, the spacetime describes screw dislocations, which can be interpreted as a combination of a screw dislocation (with $2GJ^z/\pi$ analogous to a Burgers vector) and a disclination

The governing equation for the spinor field in this curved background is the Dirac equation [15, 20–24]:

$$\left[i\gamma^\mu(x)\left(\partial_\mu - \Gamma_\mu(x)\right) - m\right]\Psi(t,x) = 0, \tag{10}$$

which differs from its flat spacetime counterpart due to the presence of the additional term $\gamma^\mu(x)\Gamma_\mu(x)$, accounting for the geometric effects introduced by the conical defect.

The generalized gamma matrices $\gamma^\mu(x)$ satisfy the Clifford algebra $\{\gamma^\mu, \gamma^\nu\} = 2g^{\mu\nu}$, and are expressed in terms of the standard Dirac matrices γ^a in Minkowski space via the tetrad fields as:

$$\gamma^\mu(x) = e^\mu_a(x)\gamma^a. \tag{11}$$

The tetrads $e^a_\mu(x)$ fulfill the orthonormality condition:

$$e^a_\mu(x)e^b_\nu(x)\eta_{ab} = g_{\mu\nu}, \tag{12}$$

where the indices $\mu, \nu = 0, 1, 2, 3$ refer to curved spacetime coordinates, and $a, b = 0, 1, 2, 3$ denote flat spacetime (tetrad) indices.

The spin connection $\Gamma_\mu(x)$ is obtained via:

$$\Gamma_\mu(x) = \frac{1}{8}\omega_{\mu ab}(x)[\gamma^a, \gamma^b], \tag{13}$$

with the spin connection one-forms $\omega_{\mu ab}$ defined as:

$$\omega_{\mu ab} = e_{a\nu}(\partial_\mu e^\nu_b + \Gamma^\nu_{\mu\lambda}e^\lambda_b). \tag{14}$$

In what follows, we will treat the three dimensional Dirac oscilltor for each case mentioned above.

A. First case: Dirac equation in a Spinning Cosmic String Background with Equal Angular Momentum and Torsion ($j^2 = 0$)

We consider the Dirac in the curved background of a spinning cosmic string with equal temporal and spatial torsion components, such that $J^t = J^z = J$, leading to a simplified torsional configuration $j^2 = 0$. The spacetime geometry is encoded in the tetrad fields:

$$e^a_\mu(x) = \begin{pmatrix} 1 & 0 & 4GJ & 0 \\ 0 & \cos\phi & -\alpha\rho\sin\phi & 0 \\ 0 & \sin\phi & \alpha\rho\cos\phi & 0 \\ 0 & 0 & 4GJ & 1 \end{pmatrix}, \quad e^\mu_a = \begin{pmatrix} 1 & 0 & -\frac{4GJ}{\alpha\rho} & 0 \\ 0 & \cos\phi & \frac{\sin\phi}{\alpha\rho} & 0 \\ 0 & -\sin\phi & \frac{\cos\phi}{\alpha\rho} & 0 \\ 0 & 0 & -\frac{4GJ}{\alpha\rho} & 1 \end{pmatrix}. \tag{15}$$

From these, we obtain the position-dependent gamma matrices in the curved spacetime:

$$\gamma^t = \gamma^0 - \frac{4GJ}{\alpha\rho}\gamma^2, \quad \gamma^\rho = \cos\phi\,\gamma^1 + \sin\phi\,\gamma^2, \quad \gamma^\phi = \frac{-\sin\phi\,\gamma^1 + \cos\phi\,\gamma^2}{\alpha\rho}, \quad \gamma^z = \gamma^3 - \frac{4GJ}{\alpha\rho}\gamma^2. \tag{16}$$

B. Second case: Dirac equation in a Purely Spinning Cosmic String Background ($J^z = 0$)

In the second configuration, we consider a purely spinning cosmic string background, where the temporal component of torsion is retained while the spatial component vanishes, i.e., $J^t \neq 0$, $J^z = 0$. The tetrad fields reduce to:

$$e^a_\mu(x) = \begin{pmatrix} 1 & 0 & 4GJ^t & 0 \\ 0 & \cos\phi & -\alpha\rho\sin\phi & 0 \\ 0 & \sin\phi & \alpha\rho\cos\phi & 0 \\ 0 & 0 & 0 & 1 \end{pmatrix}, \quad e^\mu_a(x) = \begin{pmatrix} 1 & 0 & -\frac{4GJ^t}{\alpha\rho} & 0 \\ 0 & \cos\phi & \frac{\sin\phi}{\alpha\rho} & 0 \\ 0 & -\sin\phi & \frac{\cos\phi}{\alpha\rho} & 0 \\ 0 & 0 & 0 & 1 \end{pmatrix}. \tag{17}$$

The corresponding gamma matrices become:

$$\gamma^t = \gamma^0 - \frac{4GJ^t}{\alpha\rho}\gamma^2, \quad \gamma^\rho = \cos\phi\gamma^1 + \sin\phi\gamma^2, \quad \gamma^\phi = \frac{-\sin\phi\gamma^1 + \cos\phi\gamma^2}{\alpha\rho}, \quad \gamma^z = \gamma^3. \tag{18}$$

C. Third case: Dirac equation in a Cosmic String Background with Screw Dislocations ($J^t = 0$)

In the third case, the background spacetime consists of a cosmic string with screw dislocation, where $J^t = 0$ and $J^z \neq 0$. This reflects purely spatial torsion along the z-axis. The tetrads simplify accordingly:

$$e^a_\mu(x) = \begin{pmatrix} 1 & 0 & 0 & 0 \\ 0 & \cos\phi & -\alpha\rho\sin\phi & 0 \\ 0 & \sin\phi & \alpha\rho\cos\phi & 0 \\ 0 & 0 & 4GJ^z & 1 \end{pmatrix}, \quad e^\mu_a(x) = \begin{pmatrix} 1 & 0 & 0 & 0 \\ 0 & \cos\phi & \frac{\sin\phi}{\alpha\rho} & 0 \\ 0 & -\sin\phi & \frac{\cos\phi}{\alpha\rho} & 0 \\ 0 & 0 & -\frac{4GJ^z}{\alpha\rho} & 1 \end{pmatrix}. \tag{19}$$

The corresponding gamma matrices read:

$$\gamma^t = \gamma^0, \quad \gamma^\rho = \cos\phi\gamma^1 + \sin\phi\gamma^2, \quad \gamma^\phi = \frac{-\sin\phi\gamma^1 + \cos\phi\gamma^2}{\alpha\rho}, \quad \gamma^z = \gamma^3 - \frac{4GJ^z}{\alpha\rho}\gamma^2. \tag{20}$$

D. General case: Dirac equation in a Torsion and Curvature-Modified Spacetime

We consider the dynamics of the Dirac in a nontrivial spacetime background incorporating both curvature and torsion. The metric is specified in matrix form as

$$g_{\mu\nu} = \begin{pmatrix} -1 & 0 & -4GJ^t & 0 \\ 0 & 1 & 0 & 0 \\ -4GJ^t & 0 & \alpha^2\rho^2 - 16G^2\left[(J^t)^2 - (J^z)^2\right] & 4GJ^z \\ 0 & 0 & 4GJ^z & 1 \end{pmatrix}, \tag{21}$$

This metric includes both off-diagonal and curvature-corrected diagonal components, and is consistent with cosmic string-like sources with intrinsic spin and dislocation.

To construct a spinor formalism in this background, we seek a tetrad field $e^a_\mu(x)$ satisfying $g_{\mu\nu} = e^a_\mu e^b_\nu \eta_{ab}$, where $\eta_{ab} = \mathrm{diag}(-1, 1, 1, 1)$ is the Minkowski metric in the local Lorentz frame.

A compatible choice is

$$e^a_\mu(x) = \begin{pmatrix} 1 & 0 & 4GJ^t & 0 \\ 0 & 1 & 0 & 0 \\ 0 & 0 & \alpha\rho & 0 \\ 0 & 0 & 4GJ^z & 1 \end{pmatrix}, \quad e^\mu_a(x) = \begin{pmatrix} 1 & 0 & -\dfrac{4GJ^t}{\alpha\rho} & 0 \\ 0 & 1 & 0 & 0 \\ 0 & 0 & \dfrac{1}{\alpha\rho} & 0 \\ 0 & 0 & -\dfrac{4GJ^z}{\alpha\rho} & 1 \end{pmatrix}. \tag{22}$$

From this tetrad, the curved-space Dirac matrices are constructed via $\gamma^\mu(x) = e^\mu_a(x)\gamma^a$, yielding:

$$\gamma^t = \gamma^0 - \frac{4GJ^t}{\alpha\rho}\gamma^2, \quad \gamma^\rho = \gamma^1, \quad \gamma^\phi = \frac{1}{\alpha\rho}\gamma^2, \quad \gamma^z = \gamma^3 - \frac{4GJ^z}{\alpha\rho}\gamma^2. \tag{23}$$

III. SCATTERING STATES UNDER COULOMB POTENTIAL

In this section, we formulate the Dirac equation for a massive spin-1/2 particle propagating in the curved background of a spinning cosmic string spacetime with Torsion, curvature, and a coulomb potential. The geometry induced by the cosmic string is described using cylindrical coordinates (t, ρ, ϕ, z), and the corresponding line element for a straight, rotating cosmic string endowed with torsion is given by [15–17]:

A. Pure cosmic string $J_t = J_z = 0$

We work in natural units $\hbar = c = 1$. The metric of a straight cosmic string with deficit ($\alpha \in (0, 1]$ is [25]

$$ds^2 = dt^2 - d\rho^2 - \alpha^2\rho^2 d\phi^2 - dz^2, \tag{24}$$

and the (tetrad) choice gives

$$\gamma^t = \gamma^0, \ \gamma^\rho = \gamma^1, \ \gamma^\phi = \gamma^2/(\alpha\rho), \ \gamma^z = \gamma^3 \tag{25}$$

The only nonzero spin connection component is

$$\Gamma_\phi = \frac{1-\alpha}{2}\Sigma^{12}, \qquad \Sigma^{ab} = \frac{1}{4}[\gamma^a, \gamma^b], \tag{26}$$

which produces the well-known shift in the orbital barrier (AB-like).

Add a static Coulomb vector potential

$$A_\mu = (A_t, 0, 0, 0) \tag{27}$$

with

$$A_t = -V(\rho) = -\frac{\eta}{\rho}, \qquad (\eta = Z\alpha_f \text{ in natural units, sign chosen for attraction}). \tag{28}$$

The covariant Dirac equation

$$\left[i\gamma^\mu(x)\left(\partial_\mu - ieA_\mu\right) - i\gamma^\mu(x)\Gamma_\mu(x) - m\right]\Psi = 0$$

With cylindrical symmetry,we take the separated ansatz

$$\Psi(t, \rho, \phi) = e^{-iEt} e^{il\phi} e^{ik_z z} \Big(F(\rho)\ G(\rho)\Big) \otimes \chi,$$

with constant two-spinor χ (fix a definite spin projection).

The effect of the string is to replace $(l \to l/\alpha)$ in the centrifugal piece and add the spin connection shift $(\propto (1-\alpha)\Sigma^{12})$. These combine into an α-dependent Dirac index (generalized κ)

$$\kappa(\alpha) = \pm\frac{j + \frac{1}{2}}{\alpha}, \qquad j = |l| - \tfrac{1}{2}, |l| + \tfrac{1}{2}, \ldots \tag{29}$$

(upper/lower sign for the two spinor couplings).

With

$$V(\rho) = \eta/\rho \tag{30}$$

the radial Dirac system becomes

$$\frac{dF}{d\rho} + \frac{\kappa(\alpha)}{\rho}F = \big(E + m - V(\rho)\big), G \tag{31}$$

$$\frac{dG}{d\rho} - \frac{\kappa(\alpha)}{\rho}G = \big(E - m + V(\rho)\big)F \tag{32}$$

Eliminate G to get a Schrödinger-like equation for F (similarly for G):

$$\left[-\frac{d^2}{d\rho^2} + \frac{\kappa(\alpha)\big(\kappa(\alpha) - 1\big)}{\rho^2} - \frac{2\eta E}{\rho} + \frac{2\eta\kappa(\alpha)}{\rho^2}\right]F(\rho) = k^2 F(\rho) \tag{33}$$

with the continuum wavenumber ($k \equiv \sqrt{E^2 - m^2}$) (scattering regime $E > m$). The (ρ^{-2}) term shows how α and η mix in the effective centrifugal barrier.

Introduce $z = 2k\rho$ and the standard Coulomb ansatz

$$F(\rho) = \rho^s e^{-ik\rho} w(\rho), \qquad s = \sqrt{\kappa(\alpha)^2 - 2\eta\kappa\alpha + (\eta E/k)^2}, \tag{34}$$

which yields Kummer's equation

$$z w'' + (2s + 1 - z) w' + \left(s + i\frac{\eta E}{k} \right) w = 0. \tag{35}$$

The solution regular at the origin:

$$F(\rho) = N (2k\rho)^s e^{-ik\rho} {}_1F_1 \left(s + i\frac{\eta E}{k}, 2s + 1, 2k\rho \right) \tag{36}$$

with $s \in \mathbb{R}$ if $\kappa(\alpha)^2 > (\eta E/k)^2$ (avoids supercritical complications). The companion $G(\rho)$ follows from the first-order system.

Asymptotics and phase shifts Using the large-z form of ${}_1F_1$, the spinor behaves asymptotically as outgoing/incoming spherical waves with a long-range Coulomb logarithm:

$$F(\rho) \sim \sin\left(k\rho - \frac{l\pi}{2} + \delta_l(\alpha) \right), \qquad \delta_l(\alpha) = \frac{\pi}{2}\big(|\kappa(\alpha)| - s\big) + \arg\Gamma(2s+1) - \arg\Gamma\left(s + i\frac{\eta E}{k} \right) + \frac{\eta E}{k}\ln(2k\rho). \tag{37}$$

The $\ln\rho$ piece is the universal Coulomb phase; observable quantities use renormalized (short-range) phase differences where the logarithm cancels. In the flat limit ($\alpha \to 1$) this reproduces the standard Dirac–Coulomb scattering phases.

For a central potential the spin-averaged Dirac cross section can be expressed through phase shifts. A convenient route is to separate:

- The pure Coulomb(flat) piece, which has a closed form (Mott),
- Plus the topology-induced part from ($\alpha \neq 1$) encoded in the change of partial-wave phases.

For a given energy E, so

$$k = \sqrt{E^2 - m^2} \tag{38}$$

with $\beta = k/E$, the flat-space Mott differential cross section is

$$\frac{d\sigma}{d\Omega}\bigg| = \frac{\eta^2}{4k^2\sin^4(\frac{\theta}{2})}\Big(1-\beta^2\sin^2(\tfrac{\theta}{2})\Big), \tag{39}$$

which is the relativistic correction to Rutherford. To capture the string effect we renormalize the Coulomb phases by the deficit:

$$\sigma_\ell(\eta) = \arg\Gamma(\ell+1+i\eta), \qquad \eta_{\rm rel} = \eta\frac{E}{k}. \tag{40}$$

A practical renormalized topological phase (vanishing at $\alpha = 1\}$ is

$$\delta_\ell^{\rm ren}(\alpha) = \Big[\sigma_{\ell/\alpha}(\eta_{\rm rel}) - \sigma_\ell(\eta_{\rm rel})\Big] + \frac{\pi}{2}\left(\frac{\ell+\frac{1}{2}}{\alpha} - \ell - \tfrac{1}{2}\right). \tag{41}$$

Using this in a short-range partial-wave sum gives a finite correction to the amplitude,

$$f_{\rm topo}(\theta;\alpha) = \frac{1}{2ik}\sum_{\ell=0}^{\infty}(2\ell+1)\left(e^{2i\delta_\ell^{\rm ren}(\alpha)}-1\right)P_\ell(\cos\theta) \tag{42}$$

and the total unpolarized differential cross section is modeled by

$$\frac{d\sigma}{d\Omega}(\theta,E,\alpha) = \Big|f_{\rm C}^{\rm flat}(\theta;E) + f_{\rm topo}(\theta;E,\alpha)\Big|^2\Big(1-\beta^2\sin^2\tfrac{\theta}{2}\Big), \tag{43}$$

where $f_{\rm C}^{\rm flat}$)is the standard Coulomb amplitude including the long-range phase (so that the forward $1/\sin^2(\theta/2)$ tail is exact). This construction reproduces Mott when $\alpha = 1$ and adds the α-dependent diffraction pattern through $\delta_\ell^{\rm ren}$.

Because Coulomb is long-range, the total cross section diverges from the forward region is

$$\sigma(>\theta_{\rm min}) = 2\pi\int_{\theta_{\rm min}}^{\pi}\frac{d\sigma}{d\Omega}(\theta)\sin\theta d\theta. \tag{44}$$

B. Balanced Torsion $j^2 = 0, |J_z| = |J_t| = J$

The gamma matrices include identical torsion terms for t and z (Eq. (16)), inducing a coupled energy-momentum shift. The effective $l_{eff} = l + 1/2 - 4GJ(E+k)$.

The radial system becomes:

$$\frac{dF}{d\rho} + \frac{\kappa_{\rm eff}(\alpha)}{\rho}F = (E+m-V(\rho))G, \tag{45}$$

$$\frac{dG}{d\rho} - \frac{\kappa_{\text{eff}}(\alpha)}{\rho}G = (E - m + V(\rho))F. \tag{46}$$

The second-order equation for $F(\rho)$ ($S = V$ case) is:

$$\left[-\frac{d^2}{d\rho^2} + \frac{\kappa_{\text{eff}}(\alpha)(\kappa_{\text{eff}}(\alpha) - 1)}{\rho^2} - \frac{2\eta(E + m)}{\rho}\right] F(\rho) = (E^2 - m^2)F(\rho). \tag{47}$$

The solution is

$$F(\rho) = N(2k\rho)^{\gamma} e^{-ik\rho} {}_1F_1\left(\gamma + i\eta(E + m)/k, 2\gamma + 1, 2ik\rho\right), \tag{48}$$

where

$$\gamma = \sqrt{\kappa_{\text{eff}}^2 - [\eta(E + m)/k]^2} \tag{49}$$

The phase shift is:

$$\delta_l = \frac{\pi}{2}(l - \kappa_{\text{eff}}(\alpha)) + \arg\Gamma\left(\kappa_{\text{eff}}(\alpha) + 1 - i\eta(E + m)/k\right) + \eta(E + m)/k\ln(2k\rho). \tag{50}$$

For $S = -V$, replace $\kappa_{eff} \to \kappa_{eff} + 1$ in the centrifugal term and adjust $\lambda = \eta(E - m)$.

C. Purely Spinning Cosmic String $J_z = 0$

Here, only temporal torsion contributes (Eq. (18)), yielding $l_{eff} = l + 1/2 - 4GJ_tE$ (energy-dependent frame-dragging shift, independent of k). The radial equations mirror Case 1, with $\kappa_{eff}(\alpha) = (l + 1/2 - 4GJ_tE)/\alpha$. The solution and phase shift follow identically, substituting this κ_{eff}. This case introduces rotation-induced asymmetry in scattering amplitudes, enhancing for higher E.

D. Screw Dislocations $J_t = 0$

Spatial torsion dominates (Eq. (20)), shifting $l_{eff} = l + 1/2 - 4GJ_zk$ (momentum-dependent, akin to a Burgers vector effect). The radial form is as above, with $\kappa_{eff}(\alpha) = (l + 1/2 - 4GJ_zk)/\alpha$. Phase shifts are analogous, with torsion modifying low-k states more prominently.

E. General Case: Torsion and Curvature-Modified Spacetime

For arbitrary J_t and J_z (Eq. (23)), the combined shift is $l_{eff} = l + 1/2 - 4G(J_t E + J_z k)$, encapsulating both frame-dragging and dislocation effects. The radial equation includes the radial cutoff $\rho > \rho_c = (4G/\alpha)\sqrt{(J_t)^2 - (J_z)^2}$ for $J_t)^2 > (J_z)^2$, imposing hard-wall boundary conditions at ρ_c. The phase shift gains an additional geometric contribution from ρ_c, lifting degeneracies in low-l states.

Discussion The topological defect parameters (α, J_t, J_z) alter the density of states and phase shifts, leading to modified scattering cross sections

$$\sigma = (4/k) \sum_l \sin^2 \delta_l \tag{51}$$

For small α, the phase shift has an additional Aharonov-Bohm-like contribution $\delta_{AB} \approx (1 - \alpha)\pi/4$ for Dirac particles.

The shifts in l_{eff} introduce energy- and momentum-dependent modifications to phase shifts, leading to altered cross sections $\sigma \propto \sum_l \sin^2 \delta_l$.

For small topological parameters, this yields Aharonov-Bohm-like terms

$$\delta_{AB} \approx (1 - \alpha)\pi l/2 + 2\pi G(J_t E + J_z k) \tag{52}$$

, observable in analog systems (e.g., graphene with defects mimicking strings). Torsion J_z couples to fermion chirality, potentially distinguishable from rotation J_t via polarized beams.

IV. GEOMETRIC SCATTERING IN NO ELECTROMAGNETIC POTENTIAL

With $A_\mu = 0$, the Dirac equation in the stationary, axially symmetric background reads

$$\Big[i\,\gamma^\mu(x)\big(\partial_\mu - \Gamma_\mu(x)\big) - m\Big]\Psi(x) = 0, \tag{53}$$

with

$$\gamma^\mu(x) = e^\mu{}_a(x)\gamma^a \tag{54}$$

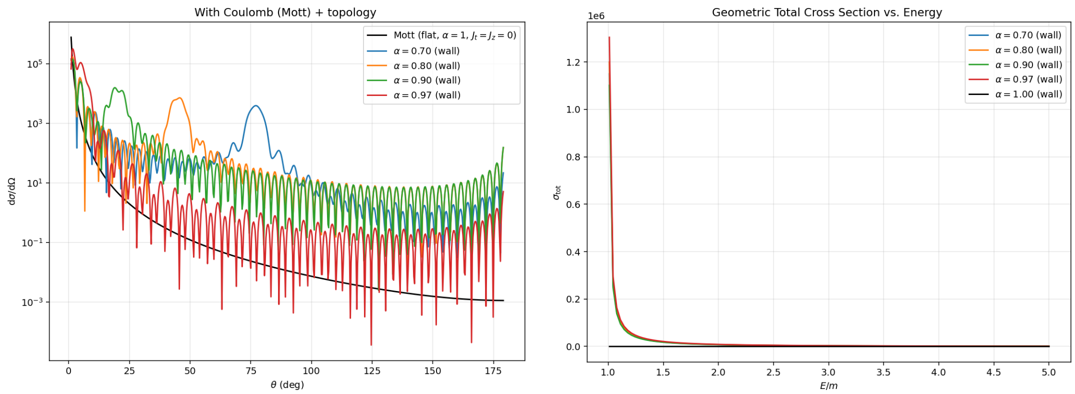

(a) Differential cross section $d\sigma/d\Omega$ versus scattering angle θ in the presence of a Coulomb potential

(b) Total cross section σ vs. energy E/m

Figure 1: Differential and Total Cross Sections for Spin-1/2 Scattering in Pure Cosmic String Spacetime (No Torsion or Rotation)

and the spin connection $\Gamma_\mu(x)$ built from a suitable tetrad $e^\mu{}_a(x)$.

We use cylindrical coordinates (t, ρ, θ, z) and the separation ansatz

$$\Psi(t, \rho, \theta, z) = e^{-iEt}\, e^{il\theta}\, e^{ik_z z} \begin{pmatrix} F(\rho) \\ G(\rho) \end{pmatrix}, \qquad l \in \mathbb{Z}. \tag{55}$$

Defining the transverse momentum k_ρ by $E^2 = m^2 + k_z^2 + k_\rho^2$, the geometric data enter through

$$\ell_{\text{eff}} = l + \tfrac{1}{2} - 4G\big(J_t E + J_z k\big), \qquad \kappa_{\text{eff}}(\alpha) = \ell_{\text{eff}}/\alpha, \qquad k = \sqrt{k_\rho^2 + k_z^2}. \tag{56}$$

Radial equations and solutions The coupled first-order radial system is

$$F'(\rho) + \frac{\kappa_{\text{eff}}(\alpha)}{\rho}\, F(\rho) = (E + m)\, G(\rho), \tag{57}$$

$$G'(\rho) - \frac{\kappa_{\text{eff}}(\alpha)}{\rho}\, G(\rho) = (E - m)\, F(\rho). \tag{58}$$

Eliminating one component yields Bessel-type equations. Introducing

$$\nu_\pm = \left|\kappa_{\text{eff}}(\alpha) \mp \tfrac{1}{2}\right|, \tag{59}$$

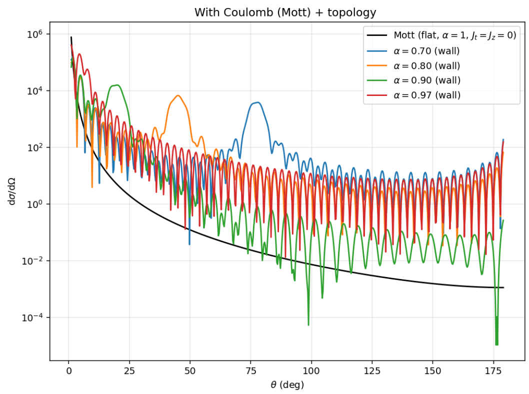

(a) Differential cross section $d\sigma/d\Omega$ versus scattering angle θ in the presence of a Coulomb potential

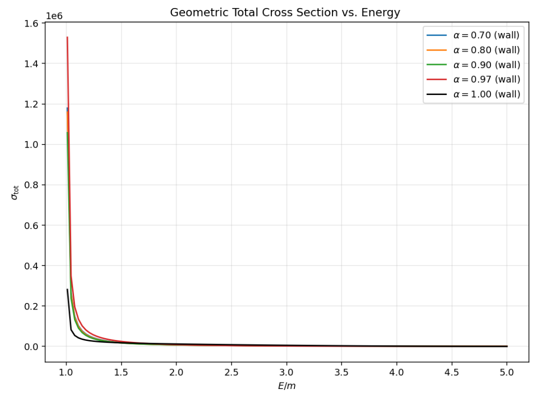

(b) Total cross section σ vs. energy E/m

Figure 2: Differential and Total Cross Sections for Spin-1/2 Scattering in Balanced Torsion Cosmic String Spacetime (J_t = J_z)

the regular radial solutions are

$$F(\rho) \propto J_{\nu_-}(k_\rho \rho), \qquad G(\rho) \propto J_{\nu_+}(k_\rho \rho). \tag{60}$$

For $J_t^2 > J_z^2$, positivity of $g_{\theta\theta}$ imposes the geometric cutoff

$$\rho > \rho_c = \frac{4G}{\alpha}\sqrt{J_t^2 - J_z^2}, \tag{61}$$

and a boundary condition at $\rho = \rho_c$ (Dirichlet is natural) must be enforced; this produces a boundary-induced phase in scattering.

Phase shifts, amplitude, and cross sections in 2D Using the large-ρ Hankel form, the partial-wave S-matrix is diagonal:

$$S_l = e^{2i\delta_l}, \qquad \delta_l(\alpha, J_t, J_z; E, k) = \frac{\pi}{2}\Big(l - \kappa_{\text{eff}}(\alpha)\Big) + \delta_{\text{wall}}(\rho_c), \tag{62}$$

where δ_{wall} arises only when the cutoff is active.

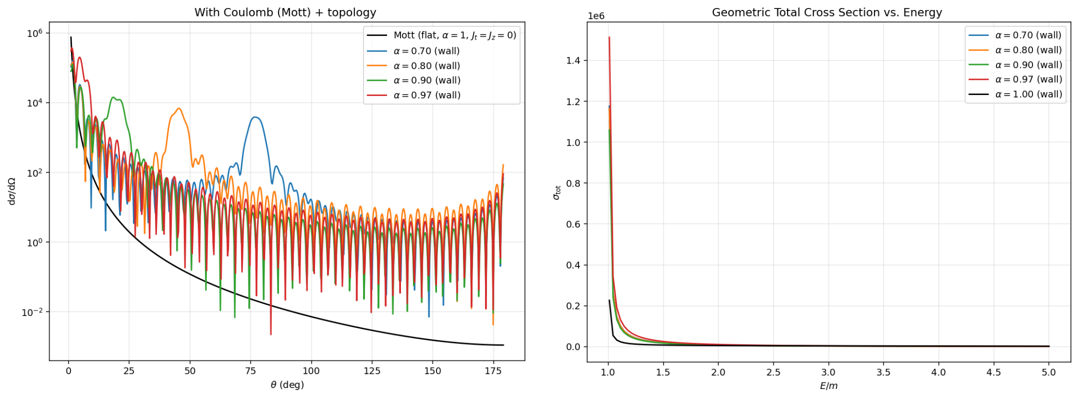

(a) Differential cross section $d\sigma/d\Omega$ versus scattering angle θ in the presence of a Coulomb potential

(b) Total cross section σ vs. energy E/m

Figure 3: Differential and Total Cross Sections for Spin-1/2 Scattering in Pure Spinning Cosmic String Spacetime (J_z = 0)

Expanding the incident plane wave in angular harmonics,

$$e^{ik_\rho \rho \cos\theta} = \sum_{l=-\infty}^{\infty} i^l J_l(k_\rho \rho)\, e^{il\theta}, \tag{63}$$

and matching outgoing pieces, the 2D scattering amplitude reads

$$f(\theta) = \frac{1}{\sqrt{2\pi k_\rho}} \sum_{l=-\infty}^{\infty} \big(S_l - 1\big) e^{il\theta} = \frac{1}{\sqrt{2\pi k_\rho}} \sum_{l=-\infty}^{\infty} \Big(e^{2i\delta_l} - 1\Big) e^{il\theta}, \tag{64}$$

with differential cross section per unit length

$$\frac{d\sigma}{d\theta} = |f(\theta)|^2, \qquad \sigma_{\rm tot} = \frac{4}{k_\rho}\, \mathrm{Im}\, f(0) = \frac{4}{k_\rho} \sum_{l=-\infty}^{\infty} \sin^2 \delta_l. \tag{65}$$

In the flat, torsionless limit $(\alpha, J_t, J_z) \to (1, 0, 0)$ one recovers free Dirac scattering. For $\alpha \neq 1$ and/or nonzero J_t, J_z, the phase \eqref{eq:phases} contains an Aharonov–Bohm–like geometric contribution, leading to characteristic forward-angle enhancement; when ρ_c is present it regularizes the near-core behavior and lifts certain low-l degeneracies..

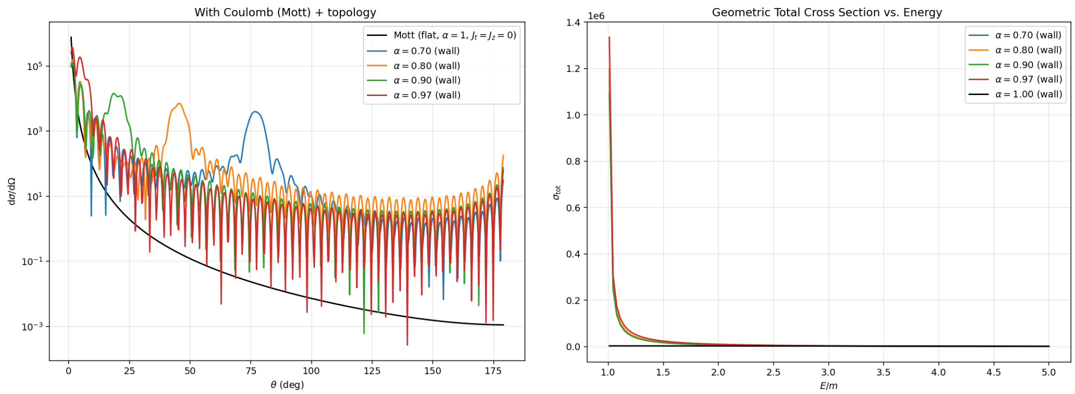

(a) Differential cross section $d\sigma/d\Omega$ versus scattering angle θ in the presence of a Coulomb potential

(b) Total cross section σ vs. energy E/m

Figure 4: Differential and Total Cross Sections for Spin-1/2 Scattering in Screw Dislocation Cosmic String Spacetime (J_t = 0)

V. RESULTS AND DISCUSSION

In this section we analyze the scattering of spin-(1/2) particles by a Coulomb potential in the spacetime of a spinning cosmic string with spacelike disclination and dislocation, and in the Coulomb-free limit where the scattering is purely geometric. The key quantity throughout is the effective azimuthal quantum number, which incorporates the conical parameter α and the angular momentum densities J_t and J_z. Its dependence on the energy E and longitudinal momentum k modifies the phase shifts and, consequently, the differential and total cross sections. The figures compare several distinct geometrical configurations to isolate the role of curvature (angular deficit), rotation, and torsion.

1. Pure cosmic string background Figure. 1 illustrates the scattering in a pure cosmic string spacetime, where only the conical defect is present and both rotation and torsion are switched off ($J_t = J_z = 0$). In this case, the effective azimuthal quantum number reduces to a purely geometric function of α, and the background is static.

Panel. 1 (a) shows the differential cross section $d\sigma/d\Omega$ as a function of the scattering angle for

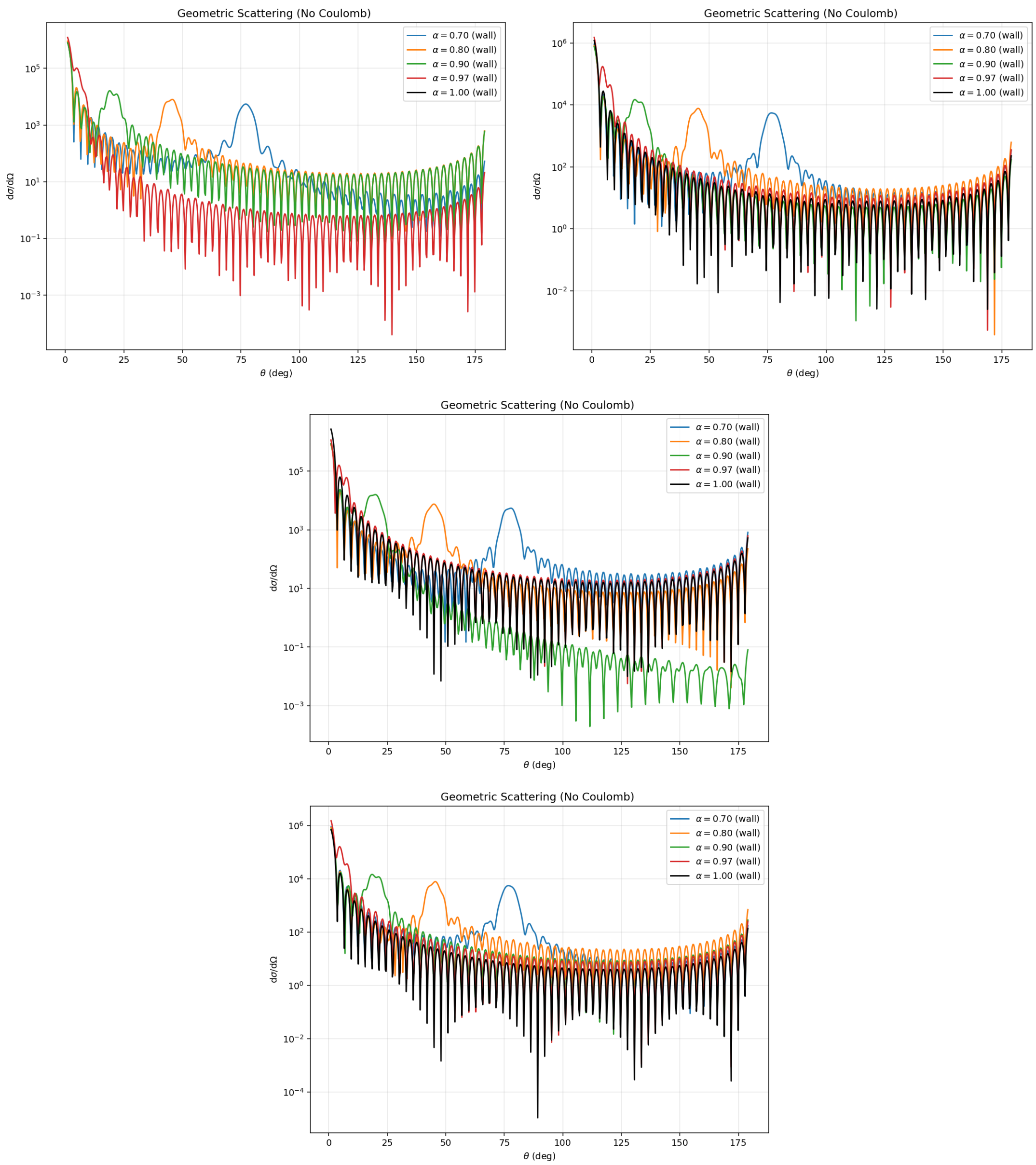

Figure 5: Spacetime Geometric Effects on Scattering Cross Sections in Four Classes of Cosmic String Models in the absence of a Coulomb potential

different values of the deficit parameter \alpha. The curves all preserve the characteristic Coulomb-dominated forward peak, reflecting the long-range nature of the interaction and reproducing the Mott behavior in the limit ($\alpha \to 1$). However, as soon as $\alpha \neq 1$, the conical geometry induces an Aharonov–Bohm–like phase in the partial waves. This appears as a shift of the interference maxima and minima with respect to the flat-space result, and as a moderate enhancement or suppression of the cross section at intermediate angles, depending on the value of α.

Panel. 1(b) displays the corresponding (cutoff) total cross section as a function of the particle energy. At low energies, the deficit angle leads to a noticeable enhancement compared to the flat case, because the geometric modification of the effective azimuthal quantum number strongly affects the lowest partial waves, which dominate in this regime. As the energy increases, the contribution of higher partial waves grows and the relative impact of the conical defect diminishes; all curves then progressively approach the flat-space behavior. Figure 1 therefore establishes the purely conical correction to Dirac–Coulomb scattering, which serves as a reference for the more general geometries considered below.

2. Balanced torsion: spinning cosmic string with ($J_t = J_z$) Figure. 2 shows the effect of balanced torsion, where rotation and torsion are present with equal strength, ($J_t = J_z = J$), while the conical defect is still controlled by α. In this case the effective azimuthal quantum number becomes an explicit function of both the energy (E and the longitudinal momentum k. As a result, the geometry is no longer a static deformation of flat space, but couples dynamically to the kinematics of the scattered particle.

The angular distributions in Fig. 2(a) exhibit much stronger distortions than in the pure-string case. The positions of the diffraction-like peaks and minima are significantly shifted, and their relative heights can be either enhanced or suppressed depending on the sign and magnitude of J. While the forward peak remains dominated by the Coulomb potential, the pattern at finite angles carries clear signatures of the balanced torsion. The comparison with Fig. 1(a) shows that this coupling to (E, k) is crucial: torsion and rotation introduce a tunable, energy-dependent geometric phase on top of the conical one.

Figure. 2(b) presents the total cross section as a function of the energy for different values of J. The overall trend is again a decrease with increasing energy, but the low-energy behavior is more sensitive than in Fig. 1. The torsion-dependent term in the effective azimuthal quantum number produces a stronger shift of the low-l phase shifts, so that the total cross section can be either amplified or reduced compared with the pure cosmic string, depending on the sign of J. This demonstrates that balanced torsion acts as an additional "control knob" to tune the Dirac–Coulomb scattering in such topologically non-trivial spacetimes.

3. Isolating rotation and dislocation effects Figures. 3 and 4 are devoted to disentangling the separate contributions of rotation J_t and screw dislocation J_z.

In Figure. 3, only the spinning character of the string is retained: $(J_t \neq 0)$ and $(J_z = 0)$. The effective azimuthal quantum number now depends on the energy E but not directly on the longitudinal momentum k. The angular distributions in Fig. 3(a) reveal an energy-dependent shift of the interference pattern induced purely by frame dragging. Compared with Figure. 1, the positions of the maxima and minima move as E changes, even for fixed α; this is the hallmark of rotational effects. The corresponding total cross section in Fig. 3(b) shows how this energy dependence modifies the high-energy tail: the decay of $\sigma_{\rm tot}(E)$ remains Coulomb-like, but its rate and normalization are noticeably altered by rotation alone.

Figure. 4, in contrast, considers a pure screw dislocation: $(J_t = 0)$ and $(J_z \neq 0)$. Here the effective azimuthal quantum number depends on the longitudinal momentum k, which encodes the influence of the Burgers-vector-like torsion. The differential cross section in Fig. 4(a) displays distortions that are most pronounced at low momenta k, where the influence of the dislocation is strongest. At higher momenta, the curves gradually approach those of the pure string, in agreement with the expectation that short wavelengths become less sensitive to the underlying torsional defect. The total cross section shown in Fig. 4(b) reflects this behavior: the largest deviations from the pure-string result occur at low energies (small (k)), while at high energies the effect of the screw dislocation becomes comparatively small.

Taken together, Figures 3 and 4 clarify that rotation J_t and screw dislocation J_z imprint qualitatively distinct signatures on both the angular and energy dependence of the cross section. Rotation primarily introduces an energy-driven phase shift, while torsion associated with the dislocation leads to a momentum-driven modification that is especially relevant at low k.

4. Geometric scattering without Coulomb interaction Finally, Figure 5 addresses the Coulomb-free limit, in which the scattering is governed solely by the geometry and topology of the spinning cosmic string spacetime. In this regime, the scattering amplitude and phase shifts reduce to purely geometric quantities, depending only on the effective azimuthal quantum number and the boundary conditions at the cylindrical cutoff.

The figure compares the differential cross sections $d\sigma/d\theta$ for the four configurations considered previously: (i) pure cosmic string, (ii) balanced torsion ($J_t = J_z$), (iii) pure spinning string ($J_t \neq 0, J_z = 0$), and (iv) pure screw dislocation ($J_t = 0, J_z \neq 0$). In the pure-string case, the conical defect alone produces an Aharonov–Bohm–like angular dependence with a forward enhancement characteristic of topological scattering. The inclusion of nonzero J_t and/or J_z introduces additional shifts in the geometric phase, leading to visible changes in the angular distributions: diffraction peaks move, their relative intensities change, and in some cases new structures appear.

This comparison highlights that even in the absence of any long-range potential, the nontrivial geometry of the spinning cosmic string spacetime is sufficient to generate rich scattering patterns. The Coulomb field, when present, superposes on these geometric effects but does not obscure them; instead, it amplifies their phenomenological relevance by providing a strong, experimentally familiar background against which the geometric distortions can be measured.

Across all figures, a consistent picture emerges: the scattering of spin-$(1/2)$ particles in a spinning cosmic string spacetime is controlled by an effective azimuthal quantum number that encodes curvature, rotation, and torsion. The conical defect α produces Aharonov–Bohm–type modifications of the Dirac–Coulomb cross section; rotation J_t and screw dislocation J_z then add energy- and momentum-dependent contributions that can significantly reshape both angular distributions and total cross sections. The Coulomb-free results confirm that these are genuinely geometric and topological effects, which persist even in the absence of conventional interactions.

VI. POTENTIAL EXPERIMENTAL IMPLEMENTATIONS

The theoretical framework presented here for Dirac scattering in spinning cosmic-string spacetimes with disclinations and dislocations has promising analogues in condensed-matter systems, where topological defects can mimic gravitational phenomena. Graphene, a two-dimensional Dirac material, is an excellent platform for realising these effects experimentally, as electrons near the

Dirac points behave as massless relativistic fermions governed by an effective Dirac equation. Meanwhile, topological defects such as disclinations (e.g. pentagonal or heptagonal rings in the honeycomb lattice) induce conical curvature analogous to the angular deficit α in cosmic strings. This leads to modified electronic states and Aharonov–Bohm-like phases. Strained or defective graphene monolayers and related Dirac metals naturally exhibit disclinations and dislocations in the honeycomb lattice that mimic conical curvature and screw-like torsion. Non-uniform strain generates pseudo-magnetic fields that reproduce the geometric and gauge structure of cosmic-string spacetimes. In this sense, the parameters α, J_t and J_z map onto lattice wedge defects, local rotations and Burgers-vector-like dislocations. Consequently, the effective azimuthal index $\kappa_{eff}(\alpha)$ and its energy/momentum dependence encode the underlying elastic and topological fields experienced by Dirac quasiparticles.

A concrete implementation would involve graphene on a conical or dislocated substrate or graphene with engineered lattice defects in the presence of a charged impurity or a gate-induced Coulomb centre. In such devices, the topology-renormalised Mott/Rutherford patterns predicted here would translate into modifications to the angular dependence of electronic scattering, and consequently to the local density of states and conductance. These could be probed using angle-resolved transport and scanning tunnelling microscopy (STM). In moiré superlattices formed by twisted bilayer graphene, emergent Dirac cones and strain fields further enrich the analogy. This allows one to simulate effective curved or expanding backgrounds, in which analogue horizons and defect structures may give rise to phenomena similar to those observed in cosmological particle production.

Similar ideas have been explored in the contexts of the Dirac oscillator and defected graphene, where strain-induced pseudo-gauge fields and torsion-like terms modify the Dirac spectrum and the scattering properties of quasiparticles. Beyond graphene, other Dirac and Weyl materials such as three-dimensional Dirac semimetals with disclination lines or screw dislocations, and topological insulators with engineered line defects offer an extended arena in which the geometric cut-off ρ_c and the separate roles of rotation J_t and torsion J_z can be investigated: line defects and helical distortions play the role of spinning/dislocated strings, while dopants or charged inclusions generate long-range Coulomb fields. Additionally, since torsion couples differently to fermion chirality than frame dragging does, spin- or valley-polarised probes could help to disentangle the contributions of J_t and J_z. This would offer a realistic way of observing the predicted geometry-induced asymmetries in a solid-state setting, thereby testing aspects of cosmic-string scattering physics on tabletop scales.

VII. CONCLUSION

In this work, we have developed a unified description of scattering states for spin-(1/2) particles in spinning cosmic-string spacetimes, in the presence of a Coulomb interaction, and in the purely geometric and spacelike disclination and dislocation limits. Starting from a general metric characterised by the deficit parameter (α), the rotational density J_t and the screw-dislocation parameter J_z, we derived the curved-space Dirac equation via the tetrad and spin-connection formalism, reducing the problem to coupled radial equations. The geometry enters the scattering problem through an effective azimuthal quantum number that depends on α, J_t, J_z, E, and k, and, in strongly rotating regimes, through a geometric radial cutoff ρ_c that removes noncausal regions and acts as a hard-wall boundary. Together, these ingredients control the phase shifts and hence the observable cross sections.

For the Coulomb problem, we obtained analytical scattering solutions in several distinct backgrounds: a pure cosmic string; a spinning string with balanced torsion $J_t = J_z$; a purely spinning string $J_z = 0$; a screw-dislocation string $J_t = 0$; and the general case. In all of these cases, the long-range Coulomb force provides the familiar Mott/Rutherford backbone, while the defect parameters impart additional Aharonov–Bohm–like phases. Our results demonstrate that the conical defect primarily generates a topology-induced modulation of the angular interference pattern and a low-energy enhancement of the total cross section. In contrast, rotation and torsion introduce genuine shifts in the effective azimuthal index that depend on energy and momentum. In particular, frame dragging associated with J_t leads to an energy-driven distortion of the angular distribution, while the screw dislocation associated with J_z produces momentum-driven modifications that are most pronounced at low k. When the cutoff ρ_c is active, an additional boundary phase emerges, eliminating low-angular-momentum degeneracies and stabilising the near-core region.

We have also analysed the Coulomb-free regime, where scattering is governed solely by spacetime geometry. In this limit, the amplitude and phase shifts reduce to purely geometric quantities; however, the resulting patterns remain highly non-trivial: the conical defect alone yields a forward enhancement and diffraction structure that is closely analogous to topological Aharonov–Bohm scattering. Meanwhile, non-zero J_t and J_z further shift and reshape the diffraction peaks. Comparing the Coulomb and non-Coulomb cases shows that the electromagnetic interaction does not obscure the geometric effects, but rather amplifies their phenomenological visibility by providing a strong, well-understood reference against which geometry-induced deviations can be identified.

Finally, we argue that these results are relevant not only to hypothetical cosmic strings in the early Universe, but also to condensed-matter analogues in Dirac materials. Strained or defective graphene, as well as three-dimensional Dirac and Weyl semimetals with line defects, can mimic the conical curvature, rotation and torsion of spinning or dislocated strings. In such systems, the effective azimuthal index and geometric cutoff translate into elastic and topological fields acting on quasiparticles. The topology-renormalised Mott/Rutherford patterns derived here correspond to measurable changes in angular-dependent electronic scattering, local density of states and transport. Future work may extend our framework to include additional interactions, such as magnetic fields or non-central potentials, investigate polarisation-resolved and time-dependent scattering and perform numerical simulations in fully dynamical string backgrounds. Such studies would further clarify the interplay between geometry, topology, and quantum scattering in astrophysical scenarios and tabletop analogue experiments.

---

[1] M. O. Katanaev, I. V. Volovich, *Anna. Phys.* **1992**, *216*, 1–28. I

[2] U. R. Fischer, M. Visser, *Phys. Revi. Lett.* **2002**, *88*, 110201.

[3] F. L. Carneiro, *Gravitational Waves in the Presence of a Cosmic String in Brans-Dicke Theory*, Preprints, **2023**, Preprint.

[4] T. W. B. Kibble, *Jour. Phys. Math. Gene.* **1976**, *9*, 1387.

[5] A. Vilenkin, *Phys. Revi. D.* **1981**, *23*, 852.

[6] A. Vilenkin, E. P. S. Shellard, *Cosmic Strings and Other Topological Defects*, Cambridge University Press, **1994**.

[7] C. J. S. Clarke, G. F. R. Ellis, J. A. Vickers, *Clas. Quan. Grav.* **1990**, *7*, 1.

[8] G. de A. Marques, V. B. Bezerra, *Phys. Revi. D.* **2002**, *66*, 105011.

[9] H. Chen, Z. W. Long, Q. K. Ran, Y. Yang, C. Y. Long, *Epl. (eur. Lett.* **2020**, *132*, 50006.

[10] A. Boumali, N. Messai, *Cana. Jour. Phys.* **2014**, *92*, 1460–1463.

[11] A. Boumali, N. Messai, *Cana. Jour. Phys.* **2017**, *95*, 999–1004.

[12] N. Messai, A. Boumali, *Euro. Phys. Jour. Plus.* **2015**, *130*, 140.

[13] N. Messai, A. Boumali, *Euro. Phys. Jour. Plus.* **2025**, *140*, 560.

[14] T. I. Rouabhia, A. Boumali, *Theo. Math. Phys.* **2023**, *217*, 1609–1619. I

[15] R. A. Puntigam, H. H. Soleng, *Clas. Quan. Grav.* **1997**, *14*, 1129–1149. I, II, II, III

[16] N. Ozdemir, *Int. J. Mod. Phys. A* **2005**, *20*, 2821—-2832. II

[17] K. Jusufi, *Euro. Phys. Jour. C.* **2016**, *76.* I, II, III

[18] R. L. L. Vitória, C. F. S. Pereira, E. V. B. Leite, A. R. Soares, H. Belich, *Inte. Jour. Mode. Phys.* **2025**, *40*, 2450176. II, II

[19] K. Bakke, V. B. Bezerra, R. L. L. Vitória, *Inte. Jour. Mode. Phys.* **2020**, *35*, 2050129. II, II

[20] Y. N. Obukhov, F. W. Hehl, *Phys. Lett. B.* **2004**, *458*, 466–470. II

[21] M. D. Pollock, *Acta. Phys. Polo. B.* **2010**, *41*, 1827–1838.

[22] S. A. Fulling, *Aspects of Quantum Field Theory in Curved Spacetime*, of *Cambridge Monographs on Mathematical Physics*, Cambridge University Press, Cambridge, **1989**.

[23] M. Nakahara, *Geometry, Topology and Physics 2nd ed.*, CRC Press, Boca Raton, **2003**, Also available under Taylor & Francis imprint.

[24] L. Parker, D. J. Toms, *Quantum Field Theory in Curved Spacetime: Quantized Fields and Gravity*, Cambridge University Press, **2009**. II

[25] J. Carvalho, C. Furtado, F. Moraes, *Phys. Revi.* **2011**, *84*, 032109. III A